Cross-tunneling and phonon bottleneck effects in the relaxation phenomena of XY pyrochlore antiferromagnet $Er_2Ti_2O_7$

M. Orendáč,[1] K. Tibenská,[2] J. Strečka,[1] J. Čisárová,[1] V. Tkáč,[1,3] A. Orendáčová,[1] E. Čižmár,[1] J. Prokleška,[3] and V. Sechovský[3]

[1]*Institute of Physics, P. J. Šafárik University, Park Angelinum 9, 041 54 Košice, Slovak Republic*

[2]*Faculty of Aeronautics, Technical University, Rampová 7, 041 21 Košice, Slovak Republic*

[3]*Faculty of Mathematics and Physics, Department of Condensed Matter Physics, Charles University, Ke Karlovu 5, 121 16 Prague 2, Czech Republic*

(Received 18 June 2015; revised manuscript received 13 October 2015; published 15 January 2016)

A multiple time scale relaxation dynamic is revealed by alternating current (ac) susceptibility studies of a single crystal of $Er_2Ti_2O_7$ performed at high temperatures ($k_BT \gg J/k_B$) in a wide range of static magnetic fields. An analysis of the frequency dependence of the ac susceptibility revealed the existence of two relaxation mechanisms, identified as an Orbach process with the pronounced effect of a phonon bottleneck and cross-tunneling. The origin of the phonon bottleneck is attributed to resonant phonon trapping. The relevance of the obtained results for relaxation phenomena found in other rare-earth pyrochlores, studied under similar conditions, is discussed.

DOI: 10.1103/PhysRevB.93.024410

I. INTRODUCTION

Geometrically frustrated magnets are intensively studied because of their unconventional static and dynamic properties arising from their inability to minimize the energy of all pairwise interactions simultaneously. Rare-earth pyrochlores, $RE_2M_2O_7$, where RE stands for a magnetic rare-earth ion and M is Ti, Mo, or Sn, represent one of the classes of materials in which frustration in three dimensions is present. In these materials, the ground states range from a classical spin ice state found in $Dy_2Ti_2O_7$ and $Ho_2Ti_2O_7$ [1,2] and quantum spin ice in $Yb_2Ti_2O_7$ [3], via spin glass of $Y_2Mo_2O_7$ formed without structural disorder [4], to various quantum spin liquids with fractionalized excitations [5,6]. Frustrated magnetic materials also feature various unusual types of order among which "order by disorder" transition in $Er_2Ti_2O_7$ received a lot of attention [7–9]. On the other hand, the origin of the absence of long-range ordering in $Er_2Sn_2O_7$ down to 100 mK has not been clarified yet [10].

Geometrical frustration also was proved to be responsible for various exotic scenarios in dynamic properties. More specifically, the reentrant, thermally activated relaxation in dipolar spin ice $Dy_2Ti_2O_7$ [11] was interpreted as the creation and annihilation of pairs of magnetic monopoles [12]. In contrast, for dynamic spin ice $Pr_2Sn_2O_7$, quantum tunneling was found to dominate the relaxation at a wide range of temperatures [13]. Persistent spin dynamics was found deep in the ordered phase of $Er_2Ti_2O_7$ at a time scale shorter than that for conventional magnets [14]. Systematic studies of a pure and magnetically diluted $Dy_2Ti_2O_7$ and $Tb_2Ti_2O_7$ performed on powdered samples [15] indicated slow spin dynamics in the polarized state, even at high temperatures ($k_BT \gg J^{\rm eff}$, where $J^{\rm eff}$ represents an effective exchange interaction). Detailed analysis ruled out a spin glass state and a simple spin-phonon relaxation among crystalline electric field (CEF) levels as explanations. The fact that relaxation tended to be suppressed by nonmagnetic doping led to a focus on the importance of correlation effects. A conjecture about the formation of small domains with a few spins oriented antiparallel to the magnetic field and slowly relaxing was formulated, however, without identifying the relaxation process. Similarly, the study of relaxation phenomena in a hybrid frustrated system $Dy_xTb_{2-x}Ti_2O_7$ revealed a more complicated temperature dependence of the imaginary component of susceptibility, with up to three anomalies depending on the x value. Subsequent construction of the temperature and Dy^{3+} content dependences of the relaxation time led to an unusually high energy barrier that could not be directly related to CEF levels of Dy^{3+} and Tb^{3+}. The underlying physical mechanism of the relaxation remained unexplained [16]. Additionally, a strong interaction of magnetic excitations and a phonon bath was proposed by the investigation of transport properties of $Gd_2Ti_2O_7$ and $Er_2Ti_2O_7$ [17].

In this paper we address the relaxation phenomena in the XY pyrochlore antiferromagnet $Er_2Ti_2O_7$ at high temperatures and a wide range of magnetic fields. Unlike previous papers [15,16] based on a study of the temperature dependence of alternating current (ac) susceptibility at various frequencies using powder samples, our investigation is focused on the analysis of frequency dependencies of the data obtained on a single crystal of $Er_2Ti_2O_7$. The analysis enabled the determination of at least two different relaxation processes, suggesting a crucial role for phonon bottleneck and cross-tunneling relaxation. We propose that these mechanisms may also be relevant in an attempt to interpret the earlier obtained high-temperature data on $Dy_2Ti_2O_7$, $Dy_xLa_{2-x}Ti_2O_7$, and $Dy_xTb_{2-x}Ti_2O_7$.

II. CRYSTAL STRUCTURE AND MAGNETIC PROPERTIES OF $Er_2Ti_2O_7$

The compound $Er_2Ti_2O_7$ represents an insulating rare-earth pyrochlore. Its structure is described by the space group $Fd\bar{3}m$ and is created by a network of corner-sharing tetrahedra with Er^{3+} ions located in the corners. The tetrahedron is characterized by four axes of quantization, each being oriented from its center to one of the corners. The magnetic Er^{3+} ion has a $4f^{11}$ electronic configuration with a $^4I_{15/2}$ ground multiplet ($L = 6$; $S = 3/2$). Apart from the electronic moment, nuclear degrees of freedom are present due to the ^{167}Er isotope with 23% abundance and nuclear spin $I = 7/2$. The values of the

 ©2016 American Physical Society

quadrupole moment $Q_{167} = 3.565$ barns and the gyromagnetic ratio $\gamma_{167} = -7.7157$ Mrad s^{-1} T^{-1} make the energy scale of quadripolar and nuclear Zeeman interactions comparable. CEF resolves 16-fold degeneracy of the electronic ground multiplet into 8 Kramer doublets. The ground state doublet can be described as an effective spin $S = 1/2$ state, since the energy levels of excited states are well separated at liquid helium temperatures. More specifically, inelastic neutron scattering performed on single crystals of $Er_2Ti_2O_7$ found the two lowest CEF levels with energies of 6.4 meV (74 K) and 7.4 meV (86 K), respectively [18]. The combined action of a crystal field and spin-orbit coupling introduces a pronounced anisotropy, which is characterized by a large difference between spectroscopic factors $g_{\rm par}$ and $g_{\rm perp}$ along and perpendicular to the axis of quantization, respectively. Detailed analysis of CEF effects in $RE_2Ti_2O_7$ compounds suggests for $Er_2Ti_2O_7$ a strong planar anisotropy with $g_{\rm par} = 1.8$ and $g_{\rm perp} = 7.7$ [19]. The calculated values reasonably agree with those proposed by the analysis of electron spin resonance spectra, $g_{\rm par} = 0.24$ and $g_{\rm perp} = 7.6$, and neutron scattering studies, $g_{\rm par} = 2.6$ and $g_{\rm perp} = 6.8$ [20]. The calculation of exchange couplings in $Er_2Ti_2O_7$ between the nearest neighbor sites performed within a spin wave approximation revealed the magnitude of the exchange coupling to be on the order of Kelvins, and the same order was found for dipolar interactions [21]. In zero magnetic field, $Er_2Ti_2O_7$ undergoes a second-order magnetic phase transition into a noncoplanar $k = 0$ antiferromagnetic structure at the critical temperature $T_N = 1.2$ K, and the magnetic state is stabilized by quantum and thermal fluctuations, classical Monte Carlo study revealed that the critical behavior corresponds to a three-dimensional XY universality class. Additionally, a quantum critical point exists for magnetic fields slightly higher than 1.5 T and oriented in the [110] direction [21].

III. EXPERIMENTAL DETAILS

A single crystal of $Er_2Ti_2O_7$ was grown by a floating zone technique using a mirror furnace [22]. A disk-shaped crystal of a nominal 1 mm thickness and 6 mm diameter used for the present investigation was cut from the bigger piece previously used in a specific heat and neutron scattering study [18]. The axis of cylindrical symmetry of the disk coincides with the [110] direction. The sample was placed in a plastic holder which was held by a straw. During the measurements, the external dc magnetic field was oriented in the [110] direction with misalignment smaller than 5 degrees. The ac susceptibility measurements were performed with a commercial magnetic property measurement system (MPMS) superconducting quantum interference device (SQUID) magnetometer (Quantum Design).

IV. RESULTS AND DISCUSSION

A. Analysis of the ac susceptibility

Alternating current susceptibility was investigated at temperatures from 2 K to 10 K and magnetic fields up to 3 T in the frequency range 0.1 Hz to 1 kHz. It should be noted that, for the selected direction of the magnetic field and $T > T_N$, the magnetization increases smoothly with gradient 1.5 μ_B/T

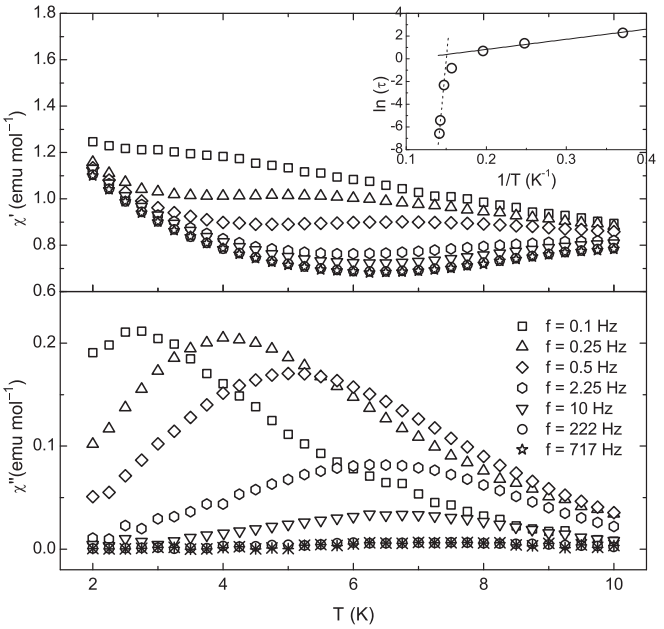

FIG. 1. Temperature dependence of real and imaginary susceptibility of $Er_2Ti_2O_7$ studied at magnetic field $B = 1.625$ T. Inset: Temperature dependence of the relaxation time analyzed at lower temperatures (solid line) and higher temperatures (dashed line). See text for a more detailed discussion.

nominally up to 2 T, and for higher magnetic fields, up to 7 T, the gradient becomes smaller, about 0.2 μ_B/T [23]. Thus, in this paper limited to 3 T, the saturated state is not reached. Following the approach from Refs. [15] and [16], the temperature dependence of ac susceptibility studied at various frequencies and magnetic fields was analyzed. The temperature dependences for selected frequencies and magnetic field 1.625 T are illustrated in Fig. 1; similar dependences were obtained in other fields. Whereas in zero magnetic field, no sensitivity to excitation frequency was detected and the imaginary component of susceptibility was found to be zero, pronounced differences for various frequencies were revealed in both the real and imaginary components of susceptibility in nonzero static magnetic fields. More specifically, real susceptibility tends to decrease with increasing temperatures for low frequencies. Higher frequencies tend to suppress the values of the real component at low temperatures, forming a minimum at about 6.5 K. The most pronounced sensitivity of the real component was found for the frequencies in hertz range.

For higher frequencies, the differences among various temperature dependences of the real component tend to diminish. The imaginary component of susceptibility displays a broad maximum, the position and magnitude of which shift with the excitation frequency. For frequencies up to 3 Hz, there is a pronounced shift of the maximum toward higher temperatures, with only a moderate decrease in its magnitude. However, at higher frequencies, the tendency is just the opposite—the position of the maximum remains nearly constant, and the maximum for higher frequencies decreases rapidly. The sensitivity of the position of the maximum in the imaginary component of susceptibility with the excitation

frequency suggests the presence of a thermally activated relaxation process. Following the approach in Ref. [16], the corresponding temperature dependence of the relaxation time constructed from the position of the maxima and the values of excitation frequencies is presented in the inset of Fig. 1 and confirms the expectation. Two regimes can be clearly distinguished, and each of them was analyzed using the Arrhenius formula,

$$\tau(T) = \tau_0 \exp\left(\frac{\Delta}{k_B T}\right), \tag{1}$$

where τ_0 represents a characteristic relaxation time, Δ denotes the activation energy, and k_B is the Boltzmann constant. The analysis yielded $\Delta_1/k_B = 8.9\,\mathrm{K}$ and $\tau_{01} = 0.38\,\mathrm{s}$ for frequencies lower than 1 Hz, whereas for frequencies higher than 5 Hz, $\Delta_2/k_B = 745\,\mathrm{K}$ and the relaxation time τ_{02} is characterized by instantaneous decay within the resolution of the measurement.

The results of the aforementioned analysis suggest a crossover between two thermally activated processes. However, this suggestion is difficult to accept. First, the values of the activation energies cannot be directly related to CEF energy levels, as in Ref. [16].

Clearly, Δ_1 is nearly an order of magnitude lower than CEF energies of the first excited doublet. Considering the values of exchange coupling and Zeeman energy, softening of the first two excited CEF modes can be safely ruled out. In contrast, the value Δ_2 seems to be overestimated. Even though an Orbach-like relaxation process can be present, it is very improbable, in that all lower energy levels would be excluded. Consequently, a different approach should be adopted. In the first step, a number of relaxation channels should be clarified. To this end, a frequency dependence of both real and imaginary components of ac susceptibility was studied in more detail. Both quantities for the temperature 4 K and all magnetic fields used are presented in Fig. 2. Similar results were obtained for other temperatures. A closer look at the obtained data reveals more complicated behavior than that proposed by the original model of Casimir and Du Pré [24].

More specifically, the real component of ac susceptibility χ' is characterized by a gradual decrease with increasing frequency; however, the decrease seems to occur in two steps, which become more pronounced for a higher magnetic field. There are two maxima in the imaginary component of ac susceptibility χ''. The first one formed for frequencies below 5 Hz, and the second one is located between 10 and 100 Hz. The first maximum tends to shift to lower frequencies with increasing magnetic field, whereas the frequency shift of the second maximum is negligible, but its value is higher. Apparently, the obtained frequency dependences suggest a coexistence of at least two relaxation processes. Thus, the data were fitted using a modified Cole-Cole equation enabling the inclusion of N relaxation processes [25],

$$\chi(\omega) = \chi_{S_N} + \sum_{n=1}^{N} \frac{\chi_{T_n} - \chi_{S_n}}{1 + (i\omega\tau_n)^{\alpha_n}}, \tag{2}$$

where $\chi_{T_n+1} = \chi_{S_n+1}$, χ_{S_n}, and χ_{T_n} represent adiabatic and isothermal susceptibilities, respectively; τ_n stands for the median relaxation time; and α_n characterizes the width of

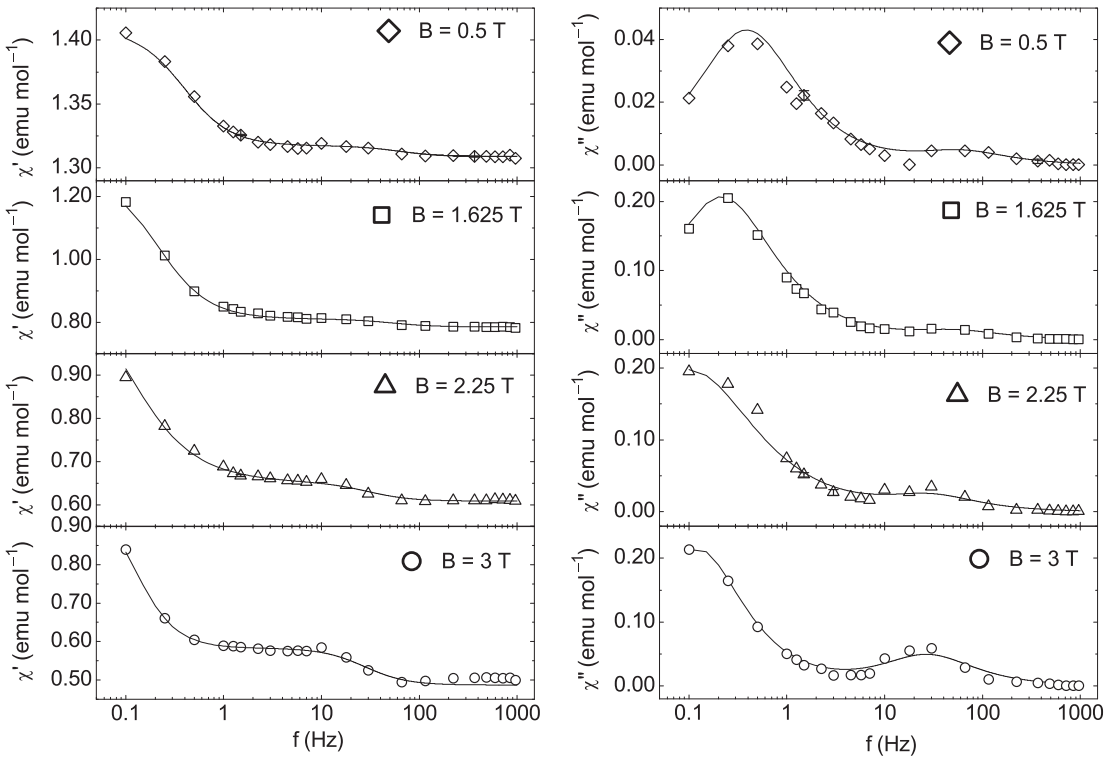

FIG. 2. Frequency dependence of real and imaginary components of ac susceptibility of $Er_2Ti_2O_7$ studied at 4 K and various magnetic fields. The error bars are comparable to the size of the symbols. The solid line represents the fit of the data using Eq. (2). See text for a more detailed discussion.

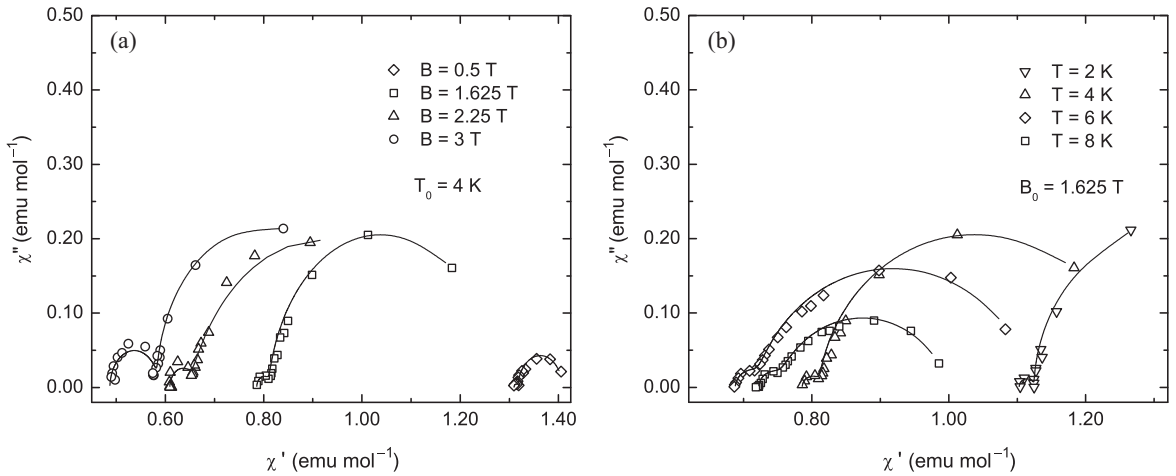

FIG. 3. Cole-Cole diagrams constructed at (a) $T_0 = 4$ K and magnetic fields 0.5 T (diamonds), 1.625 T (squares), 2.25 T (up triangles), and 3 T (circles); (b) $B_0 = 1.625$ T and temperatures 2 K (down triangles), 4 K (up triangles), 6 K (diamonds), and 8 K (squares).

the distribution function for the nth relaxation process. The value $\alpha_n = 0$ corresponds to an infinitely wide distribution of relaxation times, whereas $\alpha_n = 1$ describes Debye relaxation with a single relaxation time. As shown in Fig. 2, a reasonable agreement between the data and predictions derived from Eq. (1) was found assuming $N = 2$; therefore, in subsequent analysis, simultaneous relaxation in two channels was considered.

Recently it was proposed that if two peaks coexist in the frequency dependence of imaginary susceptibility, then alternatively, determination of the median relaxation times may be obtained from Cole-Cole diagrams [26]. Thus, to obtain more detailed information about the nature of the relaxation processes, Cole-Cole diagrams were constructed displaying the relation between χ' and χ'' for a given value of temperature and magnetic field. To illustrate the effect of the temperature and magnetic field, Cole-Cole diagrams are presented, which were constructed from the data studied at magnetic field $B_0 = 1.625$ T and various temperatures [see Fig. 3(a)] and from the data obtained at temperature $T_0 = 4$ K and various magnetic fields [see Fig. 3(b)]. The other data obtained for different values of temperatures/magnetic fields behave in a similar way. The diagrams confirm the coexistence of the two relaxation processes. The first process occurs at frequencies below 5 Hz, and χ'' associated with this process is influenced predominantly by temperature. In contrast, the second process found in the frequency range of tens of hertz tends to show temperature independence of the corresponding χ'', with a slight increase of χ'' with increasing magnetic field. In the initial step, both α_1 and α_2 were treated as free parameters. The fit yielded both values slightly higher than 1, indicating no distribution of relaxation times for both processes. Therefore in the next step, the data were reanalyzed with $\alpha_1 = \alpha_2 = 1$, and reasonable agreement was obtained. A somewhat larger deviation occurring at $B_0 = 2.25$ T and 3 T for the second relaxation process can be attributed to low values of χ'' combined with greater inaccuracy of data obtained in higher magnetic fields. The obtained result suggests the coexistence of two distinct relaxation processes, with negligible distributions of relaxation times. Therefore, a single value of relaxation time can be associated with each of the processes for a given temperature and magnetic field.

The temperature dependences of relaxation times for both processes constructed from Cole-Cole diagrams are presented in Fig. 4. It should be noted, that for $T_0 = 2$ K, only a small part of the arc associated with the first relaxation process was obtained for all magnetic fields. Therefore, the extrapolation of the arc to its maximum value leads to high inaccuracy in determining the value of the relaxation time. Obtaining more data points would require experimental studies at frequencies below 0.1 Hz, which is beyond our current experimental possibilities. Consequently, the relaxation time values at 2 K were not considered in the subsequent analysis. The obtained temperature dependences clearly suggest that the first relaxation process is thermally activated, whereas the second one is not. In contrast, the magnetic field tends to slow down the spin dynamics for both processes.

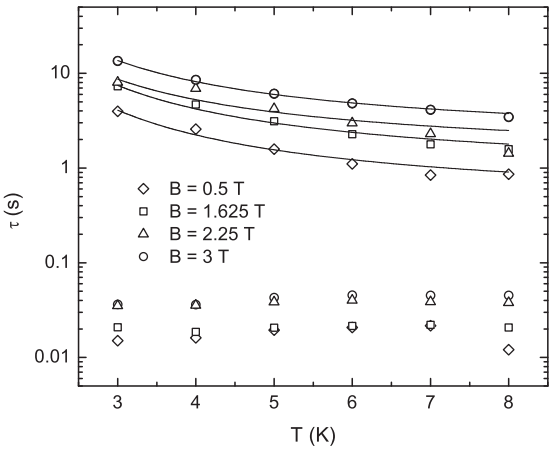

FIG. 4. Temperature dependence of the relaxation times determined from Cole-Cole diagrams at magnetic fields 0.5 T (open diamonds), 1.625 T (open squares), 2.25 T (open up triangles), and 3 T (open circles). The temperature-dependent relaxation was analyzed using predictions for the Orbach relaxation process (solid lines). See text for a more detailed discussion.

Given the ratio of the effective exchange interaction and the temperatures at which the relaxation was observed ($k_BT/J \approx 10$) the relaxation of collective degrees of freedom may not be dominant. Therefore, in the first approximation, the assumption about the relaxation of a single ion to a phonon reservoir was adopted. For a single spin relaxation, usually three processes are considered: direct ($\tau \approx T^{-1}$), Raman ($\tau \approx T^{-7}$), and Orbach [$\tau \approx \exp(\Delta/k_BT)$]. Using these predictions for the analysis of the thermally activated relaxation, only the Orbach process was found to describe the data reasonably with the parameters $\Delta/k_B = 7.2 \pm 0.6$ K, $\tau_0 = 0.37 \pm 0.04$ s; $\Delta/k_B = 6.9 \pm 0.5$ K, $\tau_0 = 0.76 \pm 0.07$ s; $\Delta/k_B = 6.0 \pm 0.6$ K, $\tau_0 = 1.2 \pm 0.1$ s; and $\Delta/k_B = 6.2 \pm 0.5$ K, $\tau_0 = 1.7 \pm 0.1$ s for magnetic fields 0.5 T, 1.625 T, 2.25 T, and 3 T, respectively. The results are presented in Fig. 4. However, the values of the energy barriers $\Delta/k_B \approx 6$–7 K obtained for various magnetic fields are more than one order of magnitude smaller than the energy of the first excited CEF level. This result indicates that a more detailed analysis of the excitation spectrum is necessary.

B. Calculation of the energy spectrum for the single tetrahedron

To search for a potential origin of the relaxation processes in $Er_2Ti_2O_7$, it is necessary to go beyond single-ion approximation. To this end, we have investigated an energy spectrum of the effective spin-1/2 tetrahedron with four different local anisotropy axes as the minimal plausible model, taking into account the nearest neighbor exchange interactions within one primitive unit cell of a pyrochlore lattice. If the magnetic field is oriented along the [110] axis, the effective spin-1/2 model of a single tetrahedron is given by the Hamiltonian [26,27]

$$\begin{aligned} H = &\sum_{j=1}^{4}\sum_{k\neq j}\left\{J_{zz}S_j^zS_k^z - J_{\pm}(S_j^+S_k^- + S_j^-S_k^+) + J_{\pm\pm}(\gamma_{jk}S_j^+S_k^+ + \gamma_{jk}^*S_j^-S_k^-) + J_{z\pm}\left[S_j^z(\zeta_{jk}S_k^+ + \zeta_{jk}^*S_k^-) + j \leftrightarrow k\right]\right\} \\ &- \sqrt{\frac{2}{3}}g_z\mu_B B\left(S_1^z - S_4^z\right) + \frac{1}{4\sqrt{3}}g_{xy}\mu_B B(S_1^+ + S_1^- - S_4^+ - S_4^-) + \frac{\sqrt{3}}{4}g_{xy}\mu_B B(S_2^+ + S_2^- - S_3^+ - S_3^-) \\ &- \frac{\mathrm{i}}{4}g_{xy}\mu_B B(S_1^+ - S_1^- - S_2^+ + S_2^- + S_3^+ - S_3^- - S_4^+ + S_4^-). \end{aligned} \tag{3}$$

Here, $S_j^{\pm} = S_j^x \pm \mathrm{i}\,S_j^y$ and $S_j^z\,(j = 1, 2, 3, 4)$ denote standard components of the spin-1/2 operator defined in four different local cubic bases [see eq. (14) in the appendix of Ref. [27]] and the respective elements of two four-by-four unimodular matrices γ_{jk} and ζ_{jk} are given by

$$\gamma_{jk} = \begin{pmatrix} 0 & 1 & \mathrm{e}^{2\pi\mathrm{i}/3} & \mathrm{e}^{4\pi\mathrm{i}/3} \\ 1 & 0 & \mathrm{e}^{4\pi\mathrm{i}/3} & \mathrm{e}^{2\pi\mathrm{i}/3} \\ \mathrm{e}^{2\pi\mathrm{i}/3} & \mathrm{e}^{4\pi\mathrm{i}/3} & 0 & 1 \\ \mathrm{e}^{4\pi\mathrm{i}/3} & \mathrm{e}^{2\pi\mathrm{i}/3} & 1 & 0 \end{pmatrix} \quad \text{and} \quad \zeta_{jk} = -\gamma_{jk}^*. \tag{4}$$

The Hamiltonian (1) of the effective spin-1/2 tetrahedron model can be rather easily numerically diagonalized, whereas the obtained energy spectrum is displayed in Fig. 5 for the model parameters (exchange couplings and g factors) reported previously as the best fitting set of inelastic neutron scattering data [27].

$$\begin{aligned} J_{\pm\pm}/k_B &= 0.487\ \text{K}, \quad J_{\pm}/k_B = 0.754\ \text{K}, \\ J_{zz}/k_B &= -0.29\,\text{K}, \quad J_{z\pm}/k_B = -0.102\ \text{K}, \\ g_{xy} &= 5.97, \quad g_z = 2.45. \end{aligned} \tag{5}$$

For the set of interaction parameters (5), the lowest energy eigenvector of the single-tetrahedron model at zero magnetic field is given by a quantum entanglement of six equally probable microstates, with two up and two down spins (i.e., the microstates with zero z component of the total spin $S_T^z = 0$, which does not significantly change its character until a level crossing around 0.45 T is reached). The lowest energy eigenstate becomes much more complex for the magnetic fields close to and above the level-crossing field, because the rising magnetic field applied along the [110] axis dramatically changes the character of this eigenstate (and also of other eigenstates) due to the admixture of the microstates with different values of S_T^z. A rather intricate nature of the lowest energy eigenvector at moderate magnetic fields is a direct consequence of a canting of local anisotropy axes of four individual spins, which in turn implies that the total spin S_T^z does not represent conserved quantity with well-defined quantum numbers, as it does not commute with the Hamiltonian. The most dominant contribution to the lowest energy eigenvector always comes from the up-up-up-down

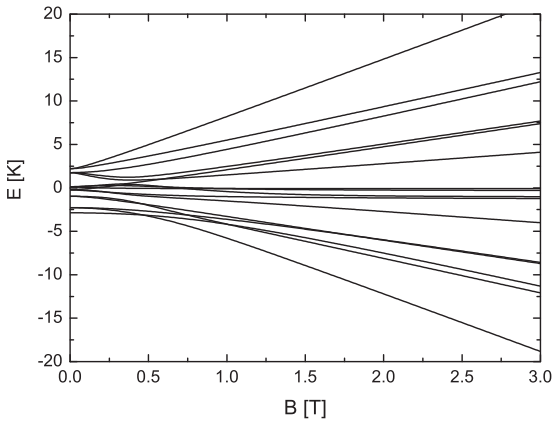

FIG. 5. The overall energy spectrum of the effective spin-1/2 tetrahedron model defined through the Hamiltonian (3) as a function of the magnetic field oriented along the [110] axis for the particular set of parameters given by Eq. (5).

microstate when the magnetic field exceeds the level-crossing field, but the other microstates with the same or a different value of S_T^z are also significantly involved in the relevant eigenvector. Owing to this fact, resonant transitions between most of eigenstates are not forbidden by the usual selection rules above the level-crossing field, and they may occur with a certain probability. It can be also seen from Fig. 5 that the overall energy spectrum is rather complicated in a low-field region, but it becomes much more evident at magnetic fields higher than 1.5 T. In the latter case, the overall energy spectrum consists of four nondegenerate energy levels and another six nearly twofold degenerate energy levels, whereas a difference between neighboring levels generally increases with the rising magnetic field, in contrast with striking nonmonotonic field dependences of energy levels observable in a low-field region.

It should be stressed, that the energy level scheme from Fig. 5 represents an oversimplified picture, yet it may give physical insight into the nature of the relaxation processes in $Er_2Ti_2O_7$ and explain gross features of the experimental data. Indeed, for all the magnetic fields used, the values of the obtained energy barriers are in reasonable agreement with the energy differences in the calculated energy spectrum. Considering that in the temperature range in which the relaxation was investigated the majority of energy levels are thermally populated and the transitions between the energy levels are allowed, thermally activated relaxation seems to be governed by the Orbach process. Despite the reasonable agreement of data and the theoretical prediction, assuming the Orbach process, small deviations persist. The number of involved energy levels may represent one of the reasons. For example, in a multilevel spin system, modified temperature dependence of the relaxation time for the Raman process was found from that proposed for the two-level system [28].

It should be noted that the values of the characteristic relaxation times τ_0 are much higher than those anticipated for the relaxation of a single spin to a phonon reservoir. Several mechanisms may be responsible for the observed feature. First, the relaxation of small clusters may lead to much longer relaxation times, as revealed by forming collective degrees of freedom in reentrant thermally activated relaxation of dipolar spin ice $Dy_2Ti_2O_7$ [11]. Second, the relaxation process may be influenced by a phonon bottleneck (PB) effect [29], which for the Orbach process leads to renormalization of the characteristic relaxation times toward higher values, keeping the magnitude of the energy gap constant [30]. For example, the relaxation time in $La_{2-x}Ce_xMg_3(NO_3)_{12} \cdot 24H_2O$ ($x = 0.002, 0.005$), where a pronounced effect of PB in the Orbach relaxation process was found, reached an order of seconds at 1.5 K [31]. On the other hand, the magnitude of the relaxation time in $La_{2-x}Ce_xMg_3(NO_3)_{12} \cdot 24H_2O$ decreased rapidly with increasing temperature, potentially due to a larger energy gap value, $\Delta/k_B \approx 37$ K. Alternatively, PB itself may not be sufficient in explaining the observed time scale of the relaxation in $Er_2Ti_2O_7$, and another mechanism needs to be considered.

Detailed theoretical and experimental studies of magnetization dynamics of Ho(III) magnetically diluted in $LiYF_4$ in a magnetic field parallel with the quantization axis confirmed an important role of nuclear degrees of freedom in the relaxation process [32]. More specifically, calculation of the spin-phonon relaxation rate of a single Ho(III) ion to a phonon bath at the temperature 2 K revealed the existence of manifold relaxation times concentrated predominantly in bands, the lowest one spanning from nominally 1 to 10 Hz. Subsequently, the phonon bottleneck was necessarily incorporated into the theoretical model for analysis of the experimental data. It may be assumed that both nuclear degrees of freedom and a phonon bottleneck may play a significant role also in the low-temperature dynamics of $Er_2Ti_2O_7$. To the best of our knowledge, the corresponding model for $Er_2Ti_2O_7$ has not been formulated. In the subsequent section, the possibility of the existence of PB in $Er_2Ti_2O_7$ will be discussed.

C. Phonon bottleneck effects

A phonon bottleneck effect becomes efficient if the energy of phonons created by relaxing spins is not directly driven to the phonon reservoir at a sufficiently short time scale. These "hot" phonons may interact with crystal boundaries and/or may be reabsorbed by adjacent spins, prolonging the reestablishment of thermal equilibrium. A phonon bottleneck effect enabled an observation of resonant tunneling of magnetization and butterfly hysteresis loops in an $S = 5/2$ dimer magnet $(Et_4N)_3Fe_2Fe_9$ [33]. Similarly, relaxation of magnetization after a microwave pulse in a Cr_7Ni single-molecule magnet was attributed to a pronounced PB effect [34]. A phonon bottleneck effect was proposed to be responsible for the slow spin relaxation revealed by our previous magnetocaloric study of the dipolar spin ice $Dy_2Ti_2O_7$ [35].

Resonant trapping of phonons may be one of the mechanisms leading to the PB effect. Trapping occurs if the energy of the resonant phonon is equal to the difference of energy levels of a magnetic ion. Then the phonon, created by a relaxing magnetic ion, may be reabsorbed by its neighbor, causing its excitation. Given that the wavelength of the phonon is much longer than the distance between the adjacent magnetic ions, the emission and subsequent absorption may become a manifold process. Coherent states are formed and the energy transfer between a spin system and lattice is prolonged [29]. In these states, neighboring spins are coherently precessing, and spin and phonon wave functions maintain defined phase relations with respect to one another. This contrasts with diffusive processes, in which phase relations are destroyed by perturbations. Spin diffusion is known to contribute to relaxation at high temperatures; its time scale is parameterized by the relaxation time $\tau_D = 1/Dk$, where D denotes the diffusion coefficient and k represents a wave vector. As far as we know, up to now, neither a theoretical nor an experimental study has addressed spin diffusion in geometrically frustrated magnetic systems. Nevertheless, experimental studies of various magnetic systems, in which spin diffusion has been proved [36–38], revealed that the corresponding characteristic relaxation times are several orders of magnitude smaller than those found in $Er_2Ti_2O_7$. Consequently, it may be assumed that spin diffusion may not be the dominant relaxation process in $Er_2Ti_2O_7$ in the time scale of interest.

Although the obtained temperature dependences of relaxation times support the presence of the PB effect in $Er_2Ti_2O_7$, before attributing the effect to the resonant phonon trapping, the assumptions necessary for the establishment of trapping

should be verified. First, trapping requires only negligible exchange coupling among magnetic ions; otherwise, the formed collective spin modes may transfer the energy of the excitation from the region in which it was originally trapped. Nevertheless, the critical T/J ratio suppressing the trapping has not been theoretically calculated. Nevertheless, the aforementioned value $k_BT/J \approx 10$ sets a reasonable background for stating that, in the situation discussed here, the effective exchange coupling represents, although nonnegligible, still a weak perturbation. It might also be considered that spin frustration may prevent paramagnons found in conventional magnets from forming above the ordering temperature, which may disturb the trapping. Second, the phonons with long wavelengths are necessary for efficient trapping [29]. In other words, the condition $k_0a_0 \ll 1$ should be met, where k_0 is momentum of the phonon involved in the trapping and a_0 represents a distance between adjacent spins. Adopting a dispersion relation for acoustic phonons and the fact that in a Debye approximation at a given temperature T_0, phonons with energies $\approx 3.8k_BT_0$ provide the greatest contribution to the lattice heat capacity [39], the following relation for k_0 can be derived,

$$\hbar k_0 v = 3.8k_BT_0 \tag{6}$$

in which v stands for the speed of sound. This quantity can be calculated from the elastic constants c_{11} and c_{44} or from Young's modulus for $Er_2Ti_2O_7$; both approaches yielded $v \approx 5500\,\mathrm{m\,s^{-1}}$ [17]. If the temperature T_0 is set, for example, to 5 K, then according to Eq. (6), $k_0 = 5.10^7\,\mathrm{m^{-1}}$ is obtained, considering the distance between neighboring Er^{3+} ions in the pyrochlore structure, $a_0 = 3.6$ Å [40], $k_0a_0 = 0.02$ is found. This result confirms that at the temperature range in which relaxation was studied, there is a large portion from the available phonons that are able to participate in the resonant trapping. It should be noted that the interaction between the coherent modes and phonons from the reservoir suppresses trapping and enhances energy transfer to the lattice. At temperatures, where decoherence effects become significant, the relaxation follows the rate characteristic for the energy transfer between a single spin and phonon reservoir. As a result, a crossover between temperature dependences of the relaxation time should occur at a temperature where phonon–phonon interactions become important. The crossover region may be deduced from the temperature dependence of thermal conductivity, κ, of an $Er_2Ti_2O_7$ single crystal [17]. The round maximum observed at about 15 K suggests that at higher temperatures, the probability of phonon–phonon collisions becomes high, causing suppression of thermal conductivity with increasing temperature. Therefore, at these temperatures, relaxation of spin to a phonon bath will dominate. In contrast, for temperatures below 10 K, phonon–phonon interactions do not represent the decisive scattering mechanism; therefore, resonant phonon trapping may occur as proposed. Consequently, the crossover may be anticipated between 10 and 15 K.

It should be noted that PB may also arise due to the interaction of hot phonons with the edges of the crystal. Such a situation occurs if the phonon mean free path becomes comparable to the dimensions of the crystal. The phonon mean free path λ can be estimated using the relation [17]

$$\kappa = \tfrac{1}{3}C_V v\lambda \tag{7}$$

in which C_V denotes a lattice-specific heat per unit volume. Considering both thermal conductivity and specific heat data obtained on good-quality $Er_2Ti_2O_7$ single crystals [17,41], λ is found to reach a value of about 0.1 mm in the Kelvin temperature range. A comparison of this value of λ with the thickness of the sample confirms that, for the $Er_2Ti_2O_7$ crystal used, scattering of phonons at the edges of the crystal is not the dominant process.

D. Cross-tunneling relaxation

Unlike the first, thermally activated relaxation, the relaxation time of the second process does not seem to be a function of temperature (Fig. 4). The magnetic field tends to increase relaxation time slightly in the whole temperature range. Absence of temperature dependence of the relaxation time is characteristic for quantum tunneling. To the best of our knowledge, the only rare-earth pyrochlore in which quantum tunneling was observed was dipolar spin ice $Dy_2Ti_2O_7$, and the tunneling was associated with a single-ion relaxation [11]. It should be stressed that planar anisotropy and the energy level scheme of a single Er^{3+} ion prevents the existence of such a type of relaxation. However, the aforementioned properties of the energy level scheme of a single tetrahedron and the corresponding states represent the necessary conditions for the onset of a *cross-tunneling relaxation* in $Er_2Ti_2O_7$. Cross-relaxation in spin systems was originally proposed by Bloembergen *et al.* [42]. Subsequently, multispin cross-relaxation in an atomic magnet represented by 0.1% of Ho^{3+}-doped $LiYF_4$ single crystal was evidenced by ac susceptibility studies at high temperatures and was attributed to weak anisotropic dipolar interactions [32,43]. As pointed out in Ref. [42], the cross-relaxation between two spins appears as if for each spin, three energy levels are present and two of them are *nearly* equal. Alternatively, one level may be approximately half of the other two. For four energy levels of a spin pair, two closely spaced doublets may be considered. A model example of cross-tunneling involves two spins, where one spin is excited from a lower to a higher state, and the other vice versa, and the energy difference is compensated by small exchange/dipolar coupling. A successful analysis of ac susceptibility data of Ho^{3+}-doped $LiYF_4$ [44] confirmed the cross-tunneling in the studied system. It was proposed that this relaxation represents an intrinsic property of a many-body system, although with weak interactions present, and may play a key role in the quantum dynamics of more complex systems, such as quantum spin glasses.

In the model considered for $Er_2Ti_2O_7$, the positions of the energy levels offer all aforementioned possibilities for the onset of cross-tunneling. The possibility of cross-tunneling also is enhanced because transitions are allowed. Additionally, considering the values of the Boltzmann occupation factor $\exp(\Delta/k_BT)$, the majority of energy levels are thermally accessible in the temperature and magnetic field range used in the experimental study. Last, but not the least, the energy level scheme in Fig. 5 will become more complex if nuclear degrees of freedom are involved. Indeed, incorporating nuclear spins

in the complex analysis of the relaxation phenomena in Ho^{3+}-doped $LiYF_4$ enabled, for each energy level, a construction of electron-nuclear sublevels with the energy separation being on the order of a hyperfine coupling constant. Consequently, the interaction between pairs of electronic spins with nuclear degrees of freedom involved led to the energy level scheme, with plenty of states between in which cross-tunneling is possible [32]. A similar situation may also be anticipated in $Er_2Ti_2O_7$ due to the nuclear magnetic moment of the ^{167}Er isotope.

V. CONCLUSIONS

Analysis of the frequency dependence of $Er_2Ti_2O_7$ ac susceptibility studied at high temperatures ($T \gg J/k_B$) revealed the existence of two distinct relaxation processes. One process is thermally activated and was associated with the Orbach process, with the pronounced effect of a phonon bottleneck. The time scale of this process is longer than that found in transition metal and rare-earth ion paramagnetic salts [45,46]. Both phonon bottleneck and nuclear degrees of freedom are proposed to help slow down the relaxation. The phonon bottleneck can be attributed to a resonant scattering of phonons, thus representing an intrinsic property of the studied material.

The other relaxation process was found to be temperature independent, indicating a tunneling mechanism. A simplified model, based on the calculation of the energy level scheme of a single tetrahedron, suggests the existence of cross-tunneling. Such a relaxation is consistent with a large number of available and thermally accessible states, with allowed transitions among them enabling all types of cross-relaxation proposed by the original model [42]. The scenario is further supported by involving nuclear degrees of freedom. Consequently, it may be proposed that for high-temperature dynamic properties of $Er_2Ti_2O_7$, frustration does not play a decisive role. Instead, single-ion effects, combined with a phonon bottleneck and cross-tunneling, may be the governing processes, much as they are for single-molecule magnets, where no frustration is present. The question arises as to how spin fluctuations persisting because of frustration may affect relaxation properties below the ordering temperature. The corresponding experimental study is in a progress.

It should be noted that two relaxation processes were also reported in a strongly frustrated hollandite vanadium oxide $V_{7.22}O_8(OH)_8Cl_{0.77}(H_3O)_{2.34}$ [47]; however, these were found in a low-temperature regime ($T \ll J/k_B$), both thermally activated, and were ascribed to the formation of spin clusters and their blocking.

The obtained results may be relevant for analyses of spin relaxation in other rare-earth pyrochlores also studied at high temperatures. More specifically, studying frequency dependence of the ac susceptibility in a wider frequency range might provide a more accurate determination of the number of relaxation channels in $Dy_xTb_{2-x}Ti_2O_7$, which subsequently could lead to a suggestion of different values of energy gaps involved in the relaxation. Notably, the slow relaxation induced by magnetic field reported in $Dy_xLa_{2-x}Ti_2O_7$ and $Dy_xTb_{2-x}Ti_2O_7$ appears at a time scale comparable to that for which cross-relaxation was found in $Er_2Ti_2O_7$. The fact that the intensity of the slow relaxation process in $Dy_xLa_{2-x}Ti_2O_7$ tends to diminish by magnetic dilution is consistent with suppressing cross-relaxation due to weakening exchange-dipolar interaction among Dy^{3+} magnetic ions. However, for $Dy_xTb_{2-x}Ti_2O_7$, the situation may be more complex due to the magnetic nature of Tb^{3+} ions and its different CEF energy level scheme. Again, systematic study of the frequency dependence of ac susceptibility may be informative.

ACKNOWLEDGMENTS

We thank D. Mc Paul for providing us the single crystal of $Er_2Ti_2O_7$ and R. Moessner for reading the manuscript and enlightening discussion. The work was supported by projects VEGA 1/0143/13, ITMS26220120005, and APVV-14-0073. The thermodynamic studies were performed in the Magnetism and Low Temperatures Laboratories of the Charles University in Prague (http://mltl.eu/), which is supported within the project of Czech Research Infrastructures (Project No. LM2011025).

[1] A. P. Ramirez, A. Hayashi, R. J. Cava, R. Siddharthan, and B. S. Shastry, Nature (London) **399**, 333 (1999).
[2] S. T. Bramwell and M. J. P. Gingras, Science **294**, 1495 (2001).
[3] L.-J. Chang, M. R. Lees, I. Watanabe, A. D. Hillier, Y. Yasui, and S. Onoda, Phys. Rev. B **89**, 184416 (2014).
[4] H. J. Silverstein, K. Fritsch, F. Flicker, A. M. Hallas, J. S. Gardner, Y. Qiu, G. Ehlers, A. T. Savici, Z. Yamani, K. A. Ross, B. D. Gaulin, M. J. P. Gingras, J. A. M. Paddison, K. Foyevtsova, R. Valenti, F. Hawthorne, C. R. Wiebe, and H. D. Zhou, Phys. Rev. B **89**, 054433 (2014).
[5] M. A. de Vries, J. R. Stewart, P. P. Deen, J. O. Piatek, G. J. Nilsen, H. M. Ronnow, and A. Harrison, Phys. Rev. Lett. **103**, 237201 (2009).
[6] T.-H. Han, J. S. Helton, S. Chu, D. G. Nocera, J. A. Rodriguez-Rivera, C. Broholm, and Y. S. Lee, Nature (London) **492**, 406 (2012).
[7] K. A. Ross, Y. Qiu, J. R. D. Copley, H. A. Dabkowska, and B. D. Gaulin, Phys. Rev. Lett. **112**, 057201 (2014).
[8] J. Oitmaa, R. R. P. Singh, B. Javanparast, A. G. R. Day, B. V. Bagheri, and M. J. P. Gingras, Phys. Rev. B **88**, 220404(R) (2013).
[9] S. Petit, J. Robert, S. Guitteny, P. Bonville, C. Decorse, J. Ollivier, H. Mutka, M. J. P. Gingras, and I. Mirebeau, Phys. Rev. B **90**, 060410(R) (2014).
[10] P. M. Sarte, H. J. Silverstein, B. T. K. Van Wyk, J. S. Gardner, Y. Qiu, H. D. Zhou, and C. R. Wiebe, J. Phys.: Condens. Matter **23**, 382201 (2011).
[11] J. Snyder, B. G. Ueland, J. S. Slusky, H. Karunadasa, R. J. Cava, A. Mizel, and P. Schiffer, Phys. Rev. Lett. **91**, 107201 (2003).
[12] L. D. C. Jaubert and P. C. W. Holdsworth, Nat. Phys. **5**, 258 (2009).

[13] H. D. Zhou, C. R. Wiebe, J. A. Janik, L. Balicas, Y. J. Yo, Y. Qiu, J. R. D. Copley, and J. S. Gardner, Phys. Rev. Lett. **101**, 227204 (2008).
[14] P. Dalmas de R'eotier, A. Yaouanc, Y. Chapuis, S. H. Curnoe, B. Grenier, E. Ressouche, C. Marin, J. Lago, C. Baines, and S. R. Giblin, Phys. Rev. B **86**, 104424 (2012).
[15] B. G. Ueland, G. C. Lau, R. J. Cava, J. R. O'Brien, and P. Schiffer, Phys. Rev. Lett. **96**, 027216 (2006).
[16] H. Xing, M. He, Ch. Feng, H. Guo, H. Zeng, and Z. A. Xu, Phys. Rev. B **81**, 134426 (2010).
[17] F. B. Zhang, Q. J. Li, Z. Y. Zhao, C. Fan, S. J. Li, X. G. Liu, X. Zhao, and X. F. Sun, Phys. Rev. B **89**, 094403 (2014) and references therein.
[18] J. D. M. Champion, M. J. Harris, P. C. W. Holdsworth, A. S. Wills, G. Balakrishnan, S. T. Bramwell, E. Čižmár, T. Fennell, J. S. Gardner, J. Lago, D. F. McMorrow, M. Orendáč, A. Orendáčová, D. McK. Paul, R. I. Smith, M. T. F. Telling, and A.Wildes, Phys. Rev. B **68**, 020401 (2003).
[19] A. Bertin, Y. Chapuis, P. Dalmas de R'eotier, and A. Yaouanc, J. Phys.: Condens. Matter **24**, 256003 (2012).
[20] S. S. Sosin, L. A. Prozorova, M. R. Lees, G. Balakrishnan, and O. A. Petrenko, Phys. Rev. B **82**, 094428 (2010).
[21] M. E. Zhitomirsky, P. C. W. Holdsworth, and R. Moessner, Phys. Rev. B **89**, 140403(R) (2014) and references therein.
[22] G. Balakrishnan, O. A. Petrenko, M. R. Lees, and D. McK. Paul, J. Phys.: Condens. Matter **10**, L723 (1998).
[23] O. A. Petrenko, M. R. Lees, and G. Balakrishnan, Eur. Phys. J. B **86**, 416 (2013).
[24] H. B. G. Casimir and P. K. Du Pré, Physica **5**, 507 (1938).
[25] M. Grahl, J. Kötzler, and I. Seßler, J. Magn. Magn. Mater. **90-91**, 187 (1990).
[26] K. A. Ross, L. Savary, B. D. Gaulin, and L. Balents, Phys. Rev. X **1**, 021002 (2011).
[27] L. Savary, K. A. Ross, B. D. Gaulin, J. P. C. Ruff, and L. Balents, Phys. Rev. Lett. **109**, 167201 (2012).
[28] R. Orbach and M. Blume, Phys. Rev. Lett. **8**, 478 (1962).
[29] D. L. Huber, Phys. Rev. **139**, A1684 (1965).
[30] P. L. Scott and C. D. Jeffries, Phys. Rev. **127**, 32 (1962).
[31] W. J. Brya and P. E. Wagner, Phys. Rev. **147**, 239 (1966).
[32] S. Bertaina, B. Barbara, R. Giraud, B. Z. Malkin, M. V. Vanuynin, A. I. Pominov, A. L. Stolov, and A. M. Tkachuk, Phys. Rev. B **74**, 184421 (2006).
[33] R. Schenker, M. N. Leuenberger, G. Chaboussant, D. Loss, and H. U. Gudel, Phys. Rev. B **72**, 184403 (2005).
[34] K. Petukhov, S. Bahr, W. Wernsdorfer, A. L. Barra, and V. Mosser, Phys. Rev. B **75**, 064408 (2007).
[35] L. R. Yaraskavitch, H. M. Revell, S. Meng, K. A. Ross, H. M. L. Noad, H. A. Dabkowska, B. D. Gaulin, and J. B. Kycia, Phys. Rev. B **85**, 020410(R) (2012).
[36] J. P. Boucher, M. A. Bakcheit, M. Nechtschein, M. Villa, G. Bonera, and F. Borsa, Phys. Rev. B **13**, 4098 (1976).
[37] R. D. Willett, F. H. Jardine, I. Rouse, R. J. Wong, Ch. P. Landee, and M. Numata, Phys. Rev. B **24**, 5372, (1981).
[38] F. Xiao, J. S. Moller, T. Lancaster, R. C. Williams, F. L. Pratt, S. J. Blundell, D. Ceresoli, A. M. Barton, and J. L. Manson, Phys. Rev. B **91**, 144417 (2015).
[39] V. Tkáč, A. Orendáčová, R. Tarasenko, E. Čižmár, M. Orendáč, K. Tibenská, A. G. Anders, S. Gao, V. Pavlík, and A. Feher, J. Phys.: Condens. Matter **25**, 506001 (2013).
[40] O. Knop, F. Brisse, L. Castelliz, and S. Sutarno, Canadian J Chem. **43**, 2812 (1965).
[41] J. P. C. Ruff, J. P. Clancy, A. Bourque, M. A. White, M. Ramazanoglu, J. S. Gardner, Y. Qiu, J. R. D. Copley, M. B. Johnson, H. A. Dabkowska, and B. D. Gaulin, Phys. Rev. Lett. **101**, 147205 (2008).
[42] N. Bloembergen, S. Shapiro, P. S. Pershan, and J. O. Artman, Phys. Rev. **114**, 445 (1959).
[43] R. Giraud, W. Wernsdorfer, A. M. Tkachuk, D. Mailly, and B. Barbara, Phys. Rev. Lett. **87**, 057203 (2001).
[44] R. Giraud, A. M. Tkachuk, and B. Barbara, Phys. Rev. Lett. **91**, 257204 (2003).
[45] A. C. de Vroomen, E. E. Lijphart, and N. J. Poulis, Physica **47**, 458 (1970).
[46] J. Soeteman, L. Bevaart, and A. J. van Duyeneveldt, Physica **74**, 126 (1974).
[47] N. A. Chernova, J. K. Ngala, P. Y. Zavalij, and M. S. Whittingham, Phys. Rev. B **75**, 014402 (2007).